Neuron
Report

Cadherin-6 Mediates Axon-Target Matching in a Non-Image-Forming Visual Circuit

Jessica A. Osterhout,[1] Nicko Josten,[2] Jena Yamada,[3] Feng Pan,[4] Shaw-wen Wu,[1] Phong L. Nguyen,[1] Georgia Panagiotakos,[2] Yukiko U. Inoue,[6] Saki F. Egusa,[6] Bela Volgyi,[4] Takayoshi Inoue,[6] Stewart A. Bloomfield,[4] Ben A. Barres,[2] David M. Berson,[5] David A. Feldheim,[3,7] and Andrew D. Huberman[1,7,*]

[1]Neurosciences Department, School of Medicine, and Neurobiology Section, Division of Biological Sciences, University of California, San Diego, La Jolla, CA 92093, USA
[2]Department of Neurobiology, Stanford University School of Medicine, Stanford, CA 94305, USA
[3]Department of Molecular, Cell and Developmental Biology, University of California Santa Cruz, Santa Cruz, CA 95064, USA
[4]Department of Physiology and Neuroscience and Ophthalmology, New York University, New York City, NY 10016, USA
[5]Department of Neuroscience, Brown University, Providence, RI 02912, USA
[6]National Institute of Neuroscience, Kodaira, Tokyo 187-8502, Japan
[7]These authors contributed equally to this work
*Correspondence: ahuberman@ucsd.edu
DOI 10.1016/j.neuron.2011.07.006

SUMMARY

Neural circuits consist of highly precise connections among specific types of neurons that serve a common functional goal. How neurons distinguish among different synaptic targets to form functionally precise circuits remains largely unknown. Here, we show that during development, the adhesion molecule cadherin-6 (Cdh6) is expressed by a subset of retinal ganglion cells (RGCs) and also by their targets in the brain. All of the Cdh6-expressing retinorecipient nuclei mediate non-image-forming visual functions. A screen of mice expressing GFP in specific subsets of RGCs revealed that Cdh3-RGCs which also express Cdh6 selectively innervate Cdh6-expressing retinorecipient targets. Moreover, in Cdh6-deficient mice, the axons of Cdh3-RGCs fail to properly innervate their targets and instead project to other visual nuclei. These findings provide functional evidence that classical cadherins promote mammalian CNS circuit development by ensuring that axons of specific cell types connect to their appropriate synaptic targets.

INTRODUCTION

Functional neural circuits consist of precise connectivity between specific sets of neurons. The assembly of such circuitry often requires that axons bypass numerous targets before selectively terminating in just one or a few specific targets. Over the last century, much progress has been made in understanding how axons undergo directed growth and pathfinding and how they form topographic maps (Sperry, 1963; Dickson, 2002; Feldheim and O'Leary, 2010). How mammalian axons identify which targets to innervate, however, remains poorly understood.

The axonal connections formed by the eyes with the brain are an attractive model for exploring mechanisms of axon-target recognition in the mammalian CNS. Retinal ganglion cells (RGCs) are the output neurons of the eye and they are divided into ~20 different types. Each RGC type encodes a different quality of the visual scene, such as brightness, direction of motion or edges (Masland, 2001; Berson, 2008), and sends that information to a limited number of retinorecipient targets that in turn regulate specific aspects of perception and behavior. For example, type 1 melanopsin RGCs encode the level of environmental illumination and project to the hypothalamic suprachiasmatic nucleus and midbrain olivary pretectal nuclei, which are involved, respectively, in entrainment of circadian rhythms and pupillary reflexes (Ecker et al., 2010; Güler et al., 2008). In contrast, the axons of alpha and On-Off direction selective RGCs innervate the dorsal lateral geniculate nucleus (dLGN) and the superior colliculus (SC) (e.g., Bowling and Michael, 1980; Tamamaki et al., 1995; Huberman et al., 2008, 2009; Rivlin-Etzion et al., 2011), targets involved in pattern vision and visually guided gaze shifts.

What mechanisms enable CNS axons to connect to specific targets and to avoid others? In the developing *Drosophila* visual system, adhesion plays a critical role in axon-target matching (Clandinin and Feldheim 2009). The cadherins are a family of molecules hypothesized to establish precise CNS connectivity by promoting selective adhesion among neurons expressing the same cadherin or combination of cadherins (Takeichi, 2007). Previous work showed that N-Cadherin is important for targeting specificity of *Drosophila* photoreceptors: loss of function mutations and experiments with genetically mosaic animals demonstrated that N-cadherin is required both in photoreceptors R1-R6 and in their target lamina neurons (Lee et al., 2001; Prakash et al., 2005). In chick, antibodies against N-cadherin disrupt laminar specific RGC axon targeting in vitro (Inoue and Sanes, 1997). Whether cadherins regulate axon-target matching in the mammalian CNS, however, remains unknown.

Here, we show that Cadherin-6 (Cdh6) is expressed by a subset of RGCs and by their retinorecipient targets in the brain, all of which mediate non-image-forming visual functions. We also show that Cdh3-GFP and Cdh6-GFP transgenic mice label the RGCs that innervate Cdh6 expressing targets. We then provide

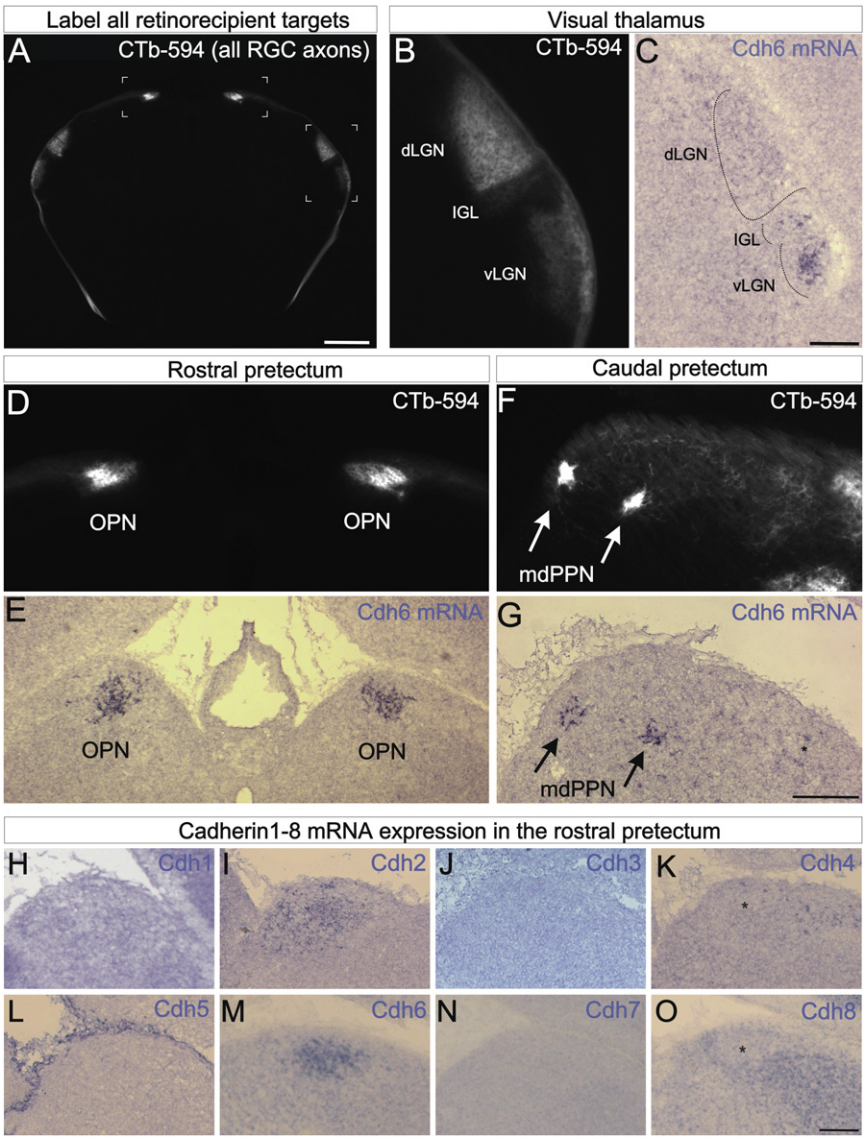

Figure 1. Cadherin-6 Is Expressed in Specific Subcortical Visual Nuclei

(A) CTb-594 labeled RGC axons at the forebrain-midbrain border of a postnatal day 2 (P2) mouse. Image is in coronal plane. Bracketed regions correspond to panels (B and D). Scale = 500 μm. (B) Pan-RGC axon labeling in the visual thalamus. The ventral lateral geniculate nucleus (vLGN), intergeniculate leaflet (IGL) and dorsal lateral geniculate nucleus (dLGN) contain RGC axons. (C) Cdh6 mRNA expressing cells in the IGL and vLGN. Scale = 100 μm. (D) CTb-594 labeled RGC axons in the rostral pretectum. The left and right olivary pretectal nuclei (OPN) are densely innervated. (E) Cdh6 mRNA expression in the OPN of a P1 mouse. (F) RGC axons in the caudal pretectum. The medial division of the posterior pretectal nucleus (mdPPN) of Scalia (1972) appear as two foci (arrows). (G) Cdh6 mRNA in the mdPPN (arrows) of a P1 mouse. Asterisk: a few Cdh6 expressing cell; these may correspond to the caudal-most OPN. Scale = (D)–(G), 250 μm. (H–O) Cdh1–8 antisense mRNA labeling in the rostral pretectum of the early postnatal mouse. Cdh2 (I) and Cdh6 (M) are expressed by the OPN, whereas Cdh4 (K) and Cdh8 (O) are expressed by cells nearby the OPN but not in the OPN itself (asterisks). Cdh1 (H), 3 (J), 5 (L), and 7 (N) are not expressed by the OPN or nearby nuclei but some of these (e.g., Cdh7) are expressed by other retinorecipient targets (not shown). (H–O) Scale = 150 μm. See also Figure S1.

genetic evidence that deletion of Cdh6 causes defects in axon-target matching in this component of the retinofugal pathway.

RESULTS

Cadherin-6 Is Expressed by a Subset of RGCs and Non-Image-Forming Visual Targets

As a first step toward assessing the role of cadherins in mammalian visual circuit assembly, we analyzed the expression patterns of several classical cadherins in the mouse brain. We visualized retinorecipient targets by making bilateral intravitreal injections of cholera toxin beta conjugated to Alexa 594 (CTb-594) which labels all RGC axons, and then compared each CTb-594 labeled target in the brain with the mRNA expression patterns of cadherin 1 (Cdh1), Cdh2, Cdh3, Cdh4, Cdh5, Cdh6, Cdh7, and Cdh8. We took particular notice of Cdh6 because it was highly and selectively expressed by a subset of the retinorecipient targets that mediate non-image-forming visual functions: the thalamic ventral lateral geniculate nucleus (vLGN), the intergeniculate leaflet (IGL) (Figures 1B and 1C), the olivary pretectal nuclei (OPN) (Figures 1D, 1E, and 1M) and the medial division of the posterior pretectal nucleus (mdPPN) (Figures 1F and 1G). The Cdh6-expressing targets relate to circadian rhythm entrainment (vLGN and IGL) (Harrington, 1997), pupil constriction (OPN) (Güler et al., 2008) and oculomotor functions (mdPPN) (Giolli et al., 2006). Cdh6 expression was specific to these targets during late embryonic and early postnatal development (~E18–P4), the stage when RGC axons innervate their targets (Godement et al., 1984) with Cdh6 expression persisting into the first postnatal week (Figure 1). The other cadherins we assayed showed patterns of expression that were notably different from Cdh6. Cdh1, 3, 4, 5, 7, and 8 were not expressed by the OPN or mdPPN although Cdh4, 7, and 8 were expressed by other retinorecipient nuclei (Figures 1H, 1J, 1K, 1L, 1N, and 1O and unpublished observations). Indeed, Cdh4 and Cdh8 were expressed by regions adjacent to and surrounding the OPN, but were absent from the OPN itself (Figures 1K and 1O). Of the cadherins we assayed, only one of them, Cdh2, was expressed by the OPN during early postnatal development, but Cdh2 was expressed by all other retinorecipient areas too (Figure 1I; data not shown). Thus, during the developmental stage when RGC axons

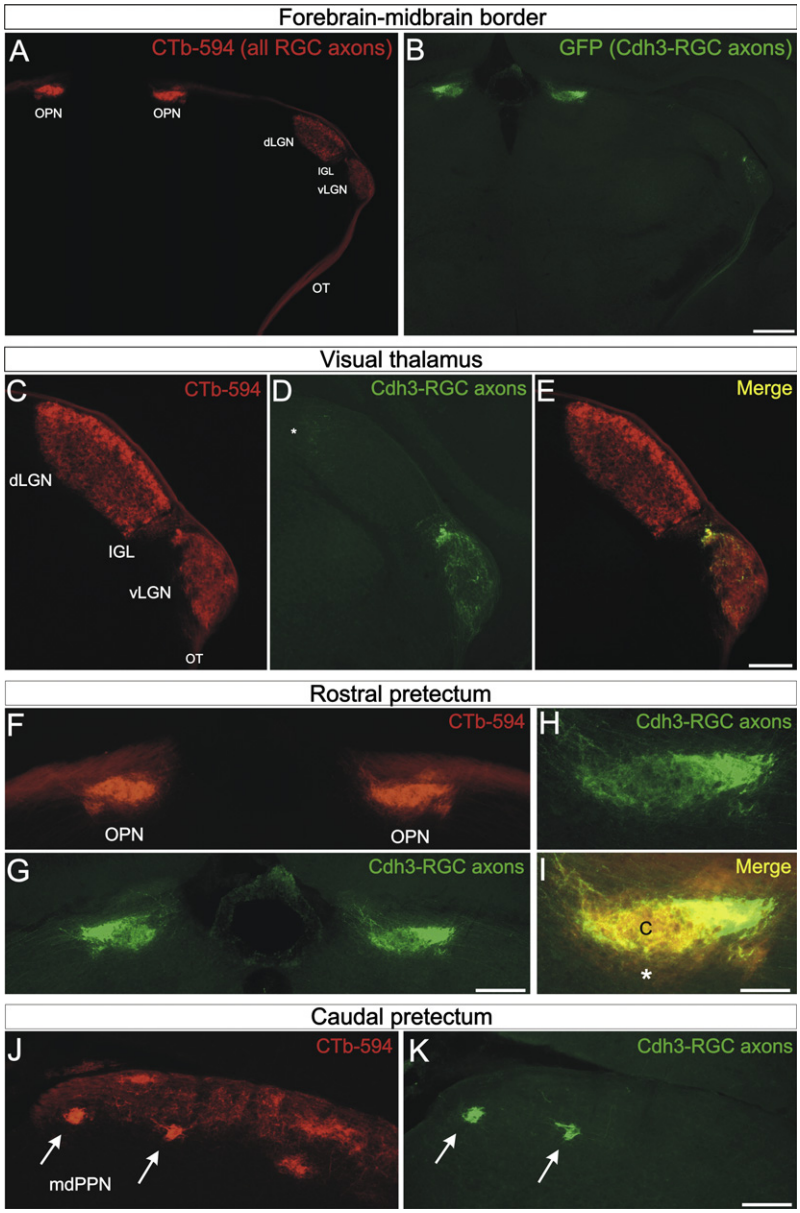

Figure 2. Cdh3-RGCs Project to Cdh6-Expressing Visual Targets

(A) CTb-594 labeled RGC axons and (B) Cdh3-GFP$^+$ RGC axons ("Cdh3-RGCs") at the level of the forebrain-midbrain border (coronal plane). The optic tract (OT), vLGN, IGL, dLGN, and OPN are apparent from CTb-594 label. (B) Cdh3-RGC axons in the OT, IGL, vLGN and OPN. Scale = 500 μm. (C–E) CTb labeled RGC axons (C), and Cdh3-RGC axons (D), and their merge (E) in the visual thalamus. Except for sparse terminals in the dorsal cap of the dLGN (asterisk), Cdh3-RGC axons selectively terminate in the vLGN and IGL. Scale = 300 μm. (F–I) Rostral pretectum OPN with (F) CTb-labeled RGC axons and (G and H) Cdh3-RGC axons and (I) their merge. (I) The OPN core ("c") is occupied by Cdh3-RGC axons, whereas the OPN "shell" (asterisk) is not and contains only CTb-594 label. Scale in (F) and (G) = 250 μm; scale in (H and I) = 100 μm. (J and K) The caudal pretectum with (J) CTb-labeled RGC axons and (I) Cdh3-RGCs axons. (J) The caudal pretectum includes many retinorecipient areas, including the mdPPN (arrows). (K) Cdh3-RGC axons selectively terminate in the mdPPN (arrows). (J and K) Scale = 175 μm. See also Figures S1–S3.

select their targets in the brain, the adhesion molecule Cdh6 is selectively expressed by a subset of non-image-forming retinorecipient targets.

Cdh3-RGCs Selectively Innervate Cdh6-Expressing Visual Targets in the Brain

To examine whether Cdh6 plays a functional role in retinofugal targeting, we needed a way to visualize the axons of the particular RGCs that innervate Cdh6 expressing visual targets. We screened a library of BAC transgenic mice (Gong et al., 2003) and found that Cdh3-GFP mice selectively label the RGCs that innervate Cdh6 expressing targets (Figure 2 and see Figure S1 available online). We injected CTb-594 into both eyes of Cdh3-GFP mice (ages P0–P20) and then examined each of those targets for the axons of Cdh3-GFP RGCs (hereafter referred to as Cdh3-RGCs). Cdh3-RGC axons terminated in the vLGN and IGL, whereas the adjacent dLGN, the target that relays visual information to the cortex for image perception, was virtually devoid of Cdh3-RGC axons (Figures 2A–2E and S1). Cdh3-RGC axons also densely innervated the OPN (Figures 2A, 2B, 2F–2I, and S1) specifically in the OPN "core," whereas the OPN "shell" was devoid of Cdh3-RGC axons (Figures 2H and 2I). A limited number of Cdh3-RGC axons remained in the optic tract until they arrived to the caudal pretectum, wherein they terminated in two dense foci corresponding to the mdPPN (Figures 2J and 2K; Scalia, 1972).

We are confident the GFP axons observed in the vLGN, IGL, OPN, and mdPPN originated from RGCs because they disappeared from those targets following eye removal (not shown). Indeed, with the exception of olfactory glia, a subset of brainstem nuclei and a small population of cells near the fourth ventricle, the brains of Cdh3-GFP mice were remarkably devoid of GFP-expressing cells (Figures 2A, 2B, S1, and S2). We found no evidence of Cdh3 mRNA expression in any retinorecipient targets (Figures 1J and S2). Together, our data indicate that Cdh3-GFP mice selectively label the RGCs that project to the vLGN, IGL, OPN, and mdPPN, the very same non-image-forming retinorecipient targets that express Cdh6.

Cdh3-RGCs Include Several Different Types, All of Which Express Cdh6

The limited number of retinorecipient targets innervated by Cdh3-RGCs prompted us to investigate which RGC types express GFP in this mouse line. Cdh3-RGCs represent ~1% of

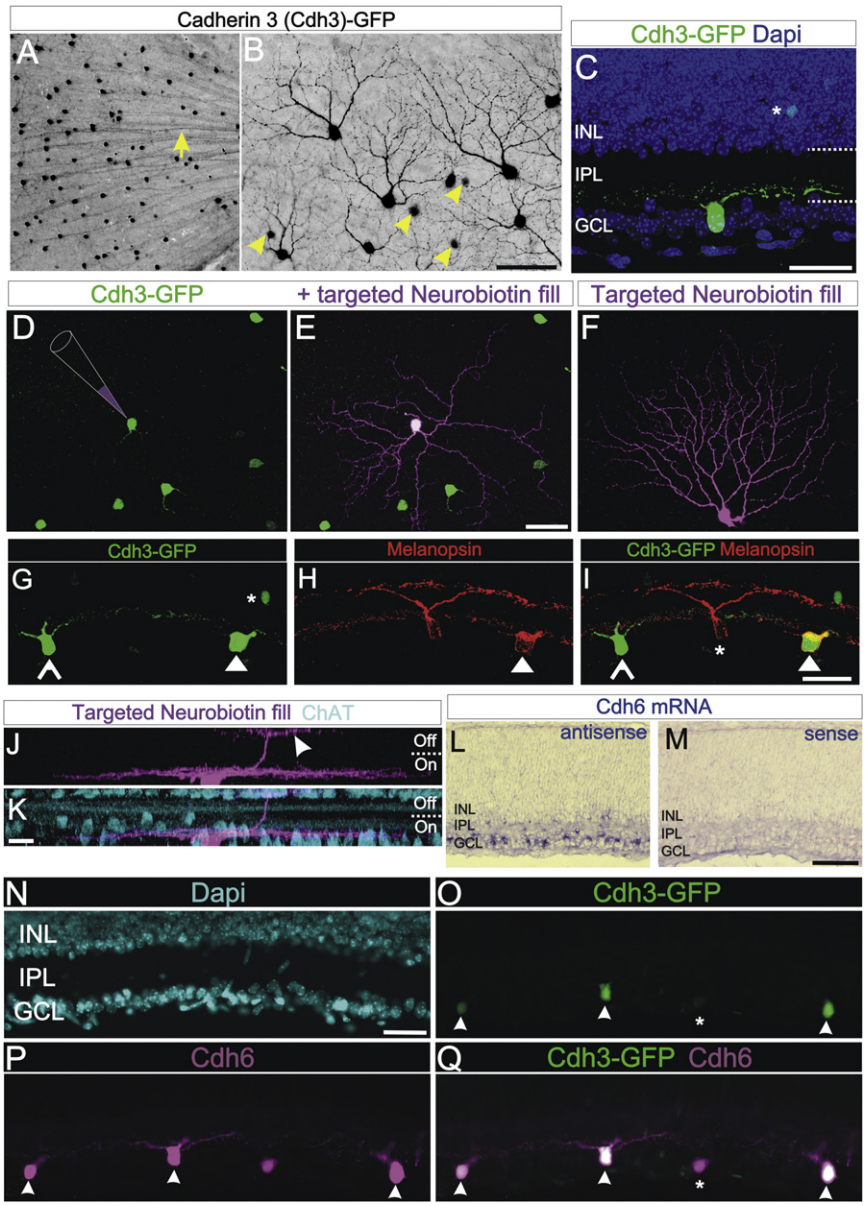

Figure 3. Cdh3-GFP and Cdh6 Expression in a Subset of Retinal Ganglion Cells

(A) GFP$^+$ somas and axons in the ganglion cell layer (GCL) of a flat mounted Cdh3-GFP retina. Arrow: GFP+ axons. (B) GFP$^+$ somas and dendrites of Cdh3-RGCs. GFP$^+$ amacrine cell somas (arrowheads) are also seen deep to the plane of focus. Scale = 200 μm (A) and 50 μm (B). (C) Cdh3-RGC in a retinal section; the cell stratifies its dendrites proximal to the GCL, in the "On" sublamina of IPL. Dashed lines: IPL boundaries. Asterisk: a GFP$^+$ amacrine. (D–F) Targeted intracellular injections with Neurobiotin (schematized in D; magenta label in E and F) reveal the morphology of individual Cdh3-RGCs. (D) Cdh3-RGCs without and (E) with injection. (E) A Cdh3-RGC with a symmetric, sparsely branched dendritic arbor. (F) A different filled Cdh3-RGC. This cell has a densely branched, asymmetric arbor (F). Scale = 50 μm (D–F). (G–I) A subset of Cdh3-RGCs express melanopsin. (G) Cdh3-RGCs (open and solid arrowheads) and an amacrine (asterisk). (H) Two RGCs and their dendrites expressing melanopsin (red). (I) Merge of (G) and (H). One of the Cdh3-RGCs expresses melanopsin (solid arrowhead) whereas the other does not (open arrowhead), a non-GFP$^+$ melanopsin RGC is also present (asterisk) Scale = 50 μm. (J and K) Confocal z stack of a Neurobiotin-filled Cdh3-RGC whose dendrites stratify mainly in the On-sublamina of the IPL. The cell extends a secondary dendritic arbor into the Off-sublamina (arrowhead). (K) ChAT stained amacrine cell bodies and dendrites (blue). Scale = 10 μm (J and K). (L and M) Cdh6 mRNA is expressed in the GCL (L) Cdh6 antisense. (M) Cdh6 sense control. Scale = 100 μm. (N–Q) Retinal section with (N) Dapi$^+$ nuclei (blue), (O) Cdh3-RGCs, and (P) Cdh6 immunoreactive cells. (Q) Merge of (O) and (P). All Cdh3-RGCs express Cdh6 (arrowheads); but some Cdh6-immunopositive cells are not Cdh3-GFP$^+$. Scale = 50 μm. See also Figure S3.

the total RGC population (mean Cdh3-RGCs per retina = 964.71 ± 57.62 GFP$^+$; n = 14 retinas; 14 mice) (Jeon et al., 1998). Morphological analysis showed that approximately half (~47%; n = 14/30) of the Cdh3-RGCs had radial, sparse dendritic arbors (Figure 3E), whereas other Cdh3-RGCs (~53%; n = 16/30) had asymmetric, densely branching dendritic arbors (Figure 3F). Also, many Cdh3-RGCs had dendrites that stratified exclusively in the On sublamina of the inner retina, (e.g., Figure 3C) whereas other Cdh3-RGCs had dendrites stratifying in both the On and Off sublamina (Figures 3J and 3K). Approximately 10% of Cdh3-RGCs also expressed the photopigment melanopsin (Figures 3G–3I). Thus, Cdh3-RGCs are not a random sampling of RGC types, nor do they comprise a single RGC type. Rather, Cdh3-RGCs include a limited number of different RGC types.

We next wanted to determine whether Cdh3-RGCs also express Cdh6. We found that Cdh6 mRNA was expressed by a subset of cells in the early postnatal RGC layer (Figures 3L and 3M), which is in agreement with a previous report (Honjo et al., 2000). Immunostaining revealed that all Cdh3-RGCs also express Cdh6 protein (Figures 3N–3Q). However, not all Cdh6 immunoreactive cells were Cdh3-RGCs (Figures 3P and 3Q), suggesting that Cdh6-RGCs represent a broader population of RGCs. Consistent with this idea, we obtained brains from Cdh6-GFP transgenic mice in which GFP is localized to axon terminals by Gap43-EGFP fusion (Inoue et al., 2009). Cdh6-RGCs heavily target the vLGN, IGL, OPN, and mdPPN, just like Cdh3-RGCs. However, Cdh6-RGCs also projected to the medial terminal nucleus (MTN) and the SC and the MTN itself expressed Cdh6 mRNA (Figure S3). Thus, Cdh3-RGCs selectively innervate Cdh6 expressing retinorecipient targets and Cdh6-RGCs project to those same targets, as well as to additional Cdh6-expressing targets.

Cadherin-6 Promotes Axon-Target Recognition in a Non-Image-Forming Visual Circuit

The most widely held view of cadherin-mediated cell-cell interactions is a homophilic model whereby cells expressing specific cadherin family members preferentially bind to cells expressing the same cadherin or combination of cadherins (Takeichi, 2007). Thus, we hypothesized that Cdh6 is involved in matching the axons of Cdh3/6-RGCs to Cdh6-expressing targets. To address this, we mated Cdh3-GFP transgenic mice to Cdh6 mutant mice (Dahl et al., 2002) to generate Cdh3-GFP::Cdh6$^{+/-}$ and Cdh3-GFP::Cdh6$^{-/-}$ mice. In early postnatal Cdh3-GFP::Cdh6$^{+/+}$ mice (n = 6 mice age P0/1; n = 6 mice age P5/6) and Cdh3-GFP::Cdh6$^{+/-}$ mice (n = 5 mice age P0/1 and n = 3 mice age P6), the axons of Cdh3-RGCs target the rostral pretectum normally and form dense oval terminal zones corresponding to the OPN (Figures 4A and 4B). Similarly, the axons of Cdh3-RGCs terminate in two dense foci in the caudal pretectum of early postnatal Cdh3-GFP::Cdh6$^{+/+}$ mice and Cdh6$^{+/-}$ mice (Figures 4D and 4E), a pattern typical of early postnatal projections to the mdPPN (Figure S1). In contrast, early postnatal Cdh3-GFP mice that lacked Cdh6 (Cdh3-GFP::Cdh6$^{-/-}$ mice) (n = 6 mice age P0/1; n = 5 mice age P6), had diminished axonal termination zones in the rostral pretectum (Figures 4C–4I). A similar lack of target recognition occurred in the caudal pretectum of Cdh3-GFP::Cdh6$^{-/-}$ mice: the axons of Cdh3-RGCs were abnormally dispersed along the margin of the optic tract and they failed to aggregate into foci typical of the early postnatal mdPPN (Figure 4F). We occasionally found Cdh3-RGC axons projecting to nonvisual midbrain areas; something we essentially never encountered in wild-type mice of the same ages (Figure 4J). In most cases, however, the Cdh3-RGC axons that failed to terminate in the OPN and mdPPN projected through and past these targets to form ectopic terminations in the more distal retinorecipient area, the SC (Figures 4G–4I). The ectopic SC terminations appeared in the deepest retinorecipient layer, the stratum opticum (asterisks in Figure 4I) or as terminal arbors in the overlying stratum griseum superficialis (Figure 4K). This stands in contrast to wild-type (Cdh6$^{+/+}$) mice where Cdh3-RGC axons are rarely observed in the SC and when they are found there, they are generally confined to the caudomedial portion of the target (Figure 4G; asterisk). Together, these data indicate that when Cdh6 is deleted, the axons of Cdh3-RGCs fail to innervate their correct targets.

One interpretation of the defective target-innervation in Cdh3-GFP::Cdh6$^{-/-}$ mice is that it reflects a failure for Cdh3-RGCs to recognize their proper targets. We can rule out two alternative interpretations. First, the reduced OPN and mdPPN innervation did not result from reduced numbers of Cdh3-RGCs in the Cdh6 mutants because they were present in normal numbers compared to wild-type mice (Cdh6$^{+/+}$: mean = 964 GFP RGCs; SEM = 57; n = 14 mice; versus Cdh6$^{-/-}$: mean = 1020 GFP RGCs; SEM = 68; n = 4 mice) (p = 0.63, two-tailed student's t test). Cadherins have been shown to play a role in sorting of motor neuron pools within the spinal cord (Price et al., 2002) which raises a second alternative interpretation of the mutant phenotype: that the axon targeting defects result from malformation of retinorecipient targets. To address this, we stained the brains of Cdh3-GFP::Cdh6$^{-/-}$ mice with antibodies to parvalbumin, which labels a population of mature OPN cells (Prichard et al., 2002). In both Cdh6$^{+/+}$ and Cdh6$^{-/-}$ mice, parvalbumin-positive neurons are arranged in a dense aggregate that delineates the basic architecture of the OPN (Figures 4L and 4M). The Cdh3-RGC axons in Cdh6$^{+/+}$ mice formed terminal arborizations throughout the parvalbumin neuron aggregates (Figure 4L), whereas in Cdh6$^{-/-}$ mice, Cdh3-RGC axons were found in only a limited, lateral portion of the parvalbumin aggregate (Figure 4M). Thus, removing Cdh6 does not disrupt the formation or positioning of OPN neurons, which argues that the defective targeting in Cdh6 mutants reflects a failure of specific RGCs to recognize and terminate in their proper targets.

We noted variation in the severity of axon targeting defects in Cdh6 mutants, especially at ages P20 and older. In early postnatal animals (P0–P6), 3 out of 11 Cdh3-GFP::Cdh6$^{-/-}$ mice exhibited apparently normal Cdh3-RGC axon targeting. In the remaining 8 Cdh3-GFP::Cdh6$^{-/-}$ mice, the reduction in Cdh3-RGC input to the OPN ranged from severe (n = 5) to moderate (n = 3). By P20, 3 out of 7 Cdh6$^{-/-}$ mice had no apparent targeting defects, 2 out of seven had severe phenotypes and 2 had moderate phenotypes. Examples of the variation in target innervation defects in the OPN and mdPPN are shown in Figure S4. This variation suggests that other molecules can compensate for early targeting errors caused by removal of Cdh6. One candidate is Cdh3. We attempted to create Cdh3-GFP::Cdh3$^{-/-}$ mice in order to visualize the axons of Cdh3-RGCs in the Cdh3 null background but unfortunately those efforts failed, likely because the Cdh3-GFP transgene and the Cdh3 null cassette are located near one another on the same chromosome. However, whole-eye retinofugal tracing of Cdh3$^{-/-}$ mutant mice indicated that eye-specific targeting to the dLGN and SC was normal. Input to image-forming areas was also normal in Cdh6$^{-/-}$ mutant mice, as assessed by whole-eye anterograde labeling (Figures 4N–4P).

DISCUSSION

Deciphering the molecular basis of neural circuit specificity is a longstanding goal of neurobiology. The hypothesis that cadherins generate precise connectivity in the nervous system was initially put forth by Takeichi and coworkers (Suzuki et al., 1997; Inoue et al., 1998). Loss-of-function data support that model in lower vertebrates and flies (Inoue and Sanes, 1997; Lee et al., 2001; Prakash et al., 2005). Previous studies showed that distinct components of mammalian sensory circuits can be defined by their expression of different cadherins (Suzuki et al., 1997; Hertel et al., 2008), but evidence that cadherins play a functional role in generating wiring specificity in the mammalian CNS has been lacking. Here, we showed that Cdh6 mediates axon-target matching in a specific non-image-forming visual circuit. These data provide some of the first evidence that a specific classical cadherin can promote wiring specificity in the mammalian visual system.

The axon targeting defects we observed in Cdh6 knockout mice raise important questions about the mechanisms by which cadherins impart specificity of neural connections. The simplest explanation is that Cdh6-expressing RGC axons adhere to Cdh6 expressing target neurons via homophilic interactions that occur at the level of the targets. The ability of cadherins to localize to

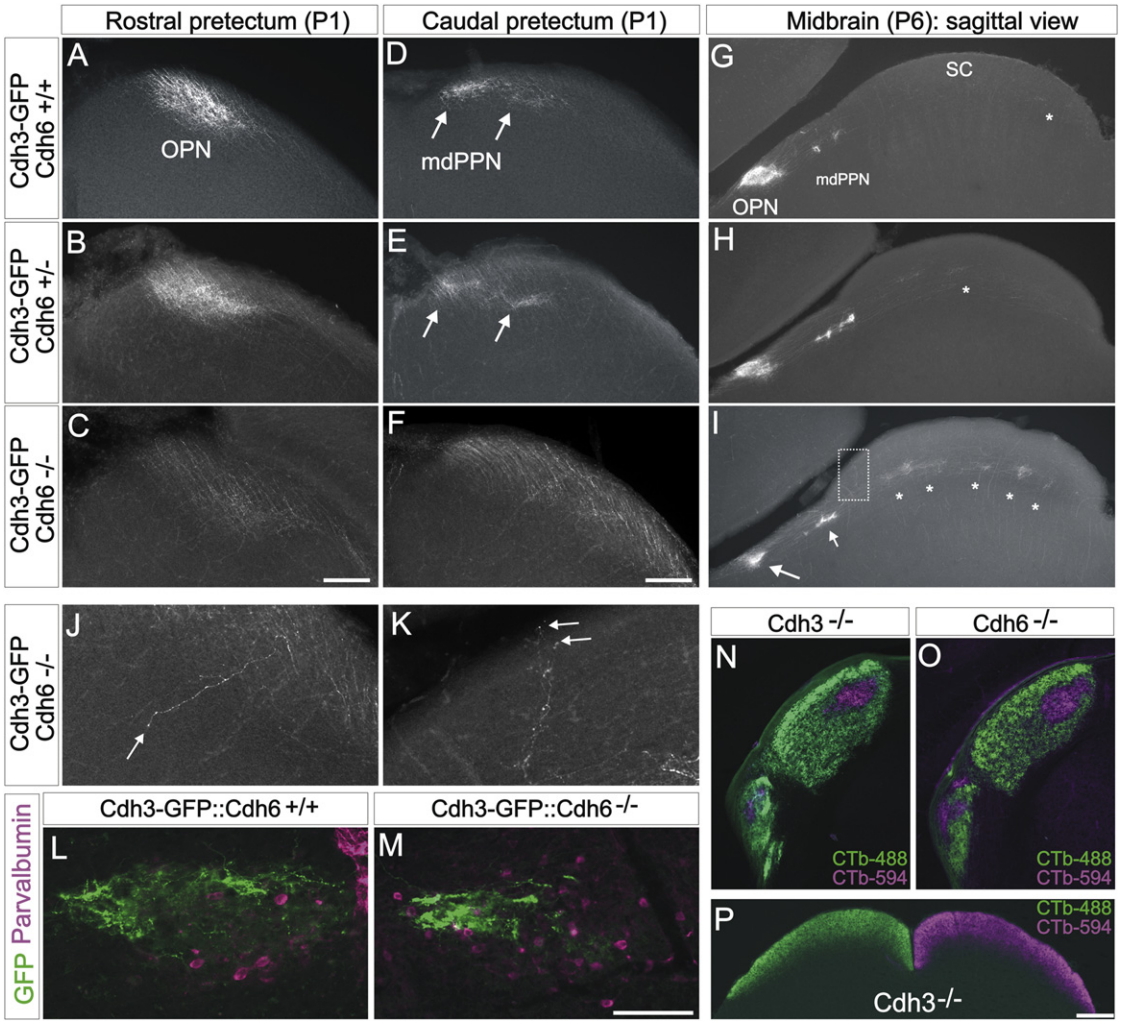

Figure 4. Cdh3-RGCs Display Target Recognition Errors in Cdh6 Knockout Mice

(A–F) Coronal view of Cdh3-RGC axon projections to the rostral (A–C) and caudal (D–F) pretectum of P1 mice. (A and D) Cdh3-GFP:Cdh6$^{+/+}$, (B and E) Cdh3-GFP:Cdh6$^{+/-}$, (C and F) Cdh3-GFP:Cdh6$^{-/-}$ mice. In Cdh6$^{+/+}$ and Cdh6$^{+/-}$ mice, an oval termination zone characteristic of the OPN is apparent, whereas in Cdh6$^{-/-}$mice, Cdh3-RGC axons fail to terminate in the OPN region. In Cdh3-GFP:Cdh6$^{+/+}$ mice (D) and Cdh3-GFP:Cdh6$^{+/-}$ mice (E), two foci of GFP^{+} axon terminals are seen (arrows) whereas the Cdh3-GFP:Cdh6$^{-/-}$ mice (F) lack these foci; instead Cdh3-RGC axons course through the caudal pretectum. Scale = 100 μm (A–F). (G–I) Sagittal view of Cdh3-RGC axons in the pretectum and SC of P6 Cdh3-GFP:Cdh6$^{+/+}$ (G), Cdh3-GFP:Cdh6$^{+/-}$ (H), and Cdh3-GFP:Cdh6$^{-/-}$ (I) mice. In Cdh3-GFP:Cdh6$^{+/+}$ mice, Cdh3-RGC axons form a dense oval termination in the OPN and foci in the mdPPN; sparse axons are observed in the SC (asterisk). (H) In Cdh3-GFP:Cdh6$^{+/-}$ mice, Cdh3-RGC axons terminate in OPN and in the mdPPN and SC. (I) In Cdh3::Cdh6$^{-/-}$ mice, Cdh3-RGC axons display diminished terminal fields in the OPN region (larger arrow) and mdPPN (small arrow); asterisks: ectopic terminations in the SC. Scale = 500 μm (G–I). (J and K) High-magnification view of Cdh3-RGC axons mistargeting in the OPN region (J) and in the rostral SC (K; from boxed region in I). Arrow in (J): a rare case of an axon seen projecting through the OPN region along the lateral-medial axis. Most misprojecting mutant axons travel through and past the OPN region along the rostral-caudal axis (as in C, F, and I, and see Figure S4). (L and M) Parvalbumin expressing OPN neurons (magenta) of P20 Cdh6$^{+/+}$and P20 Cdh6$^{-/-}$ mouse. Cdh3-RGC axons are found in the target cell region of both genotypes, but in Cdh6$^{-/-}$ mice, they terminate in a lateral zone (M), rather than diffusely filling the entire aggregate of parvalbumin cells. Scale = 150 μm. See main text and Figure S4 for quantitative details on phenotypic variation and examples of Cdh6 mutants. (N and O) Whole-eye anterograde labeling of RGC axons from the contralateral (CTb-488; green) and ipsilateral (CTb-594; magenta) eye in the visual thalamus (N and O) of a Cdh3$^{-/-}$ and a Cdh6$^{-/-}$ mouse. RGC axons are confined to their normal targets, the dLGN, IGL and vLGN (see Figures 1 and 3 for nuclei locations) and normal positioning of RGC axons is observed. (P) Eye-specific projections to the SC in a Cdh3$^{-/-}$ mouse. Scale = 250 μm.

synapses (Takeichi, 2007) supports that model. Alternatively, homophilic interactions among Cdh6 expressing RGCs may occur along the length of axons, en route to their targets. However, if the latter were the case, then we might expect to see defasciculation or axon growth deficiencies in Cdh6 mutants along the retinofugal pathway. We did not observe this; Cdh6 mutant axons arrived at their targets and indeed grew through and past them. They simply failed to terminate within those targets (e.g., Figures 4A–4I).

An alternative explanation is that the Cdh6 mutants phenotypes arise from heterophilic interactions among different cadherins. We did not examine Cdh6 binding specificity in this study,

but the expression of Cdh3 and Cdh6 in a single cohort of RGCs that innervate common targets (Figures 1–3), and the fact that Cdh2 is coexpressed with Cdh6 in those targets (Figures 1I and 1M), raises the possibility these cadherins generate target specificity by heterophilic interactions. The presence of multiple cadherins in the same neurons may also help explain why the Cdh6 null is not a fully penetrant phenotype: one cadherin may substitute in the others absence to reinforce proper axon-target connectivity. It is worth noting that age-dependent variability in phenotypes was also observed for kidney development in Cadherin-6 mutants (Mah et al., 2000).

Although not a fully penetrant phenotype, the absence of Cdh6 caused dramatic axon targeting defects in many cases, especially in early postnatal mice (Figures 4 and S4). The nature of those defects is informative toward understanding how cadherins impart specificity of connections: it was rare to observe mutant axons forming ectopic connections away from but in the vicinity of their normal targets. More often, the mutant axons traveled through their normal targets until they reached a different visual target, the SC. The fact that Cdh6 mutant axons grow through their targets but fail to stop and elaborate terminal arbors within them, supports the idea that removal of Cdh6 does not alter axon growth or guidance per se. Rather, Cdh6 appears necessary for axons to stop in the correct targets. The observation that misprojecting axons were able to invade the SC and form clustered terminations there (Figure 4I) also suggests that Cdh6 mutant axons are still capable of forming synapses. The location of those synapses is likely constrained by the guidance and activity dependent mechanisms that control afferent organization within that target, such as ephrins and spontaneous activity (Feldheim and O'Leary, 2010). Indeed, the retino-SC defects observed in Cdh6 mutants are reminiscent of the phenotypes observed in surgical "rewiring experiments" where RGC axons are forced into auditory nuclei. In those experiments, the misrouted RGC axons adopt terminal fields that are shaped by the local architecture and ephrin-based guidance systems they confront within the novel targets (Ellsworth et al., 2005).

Our data showing that an adhesion molecule is important for visual system wiring are consistent with previous reports showing that adhesion regulates RGC axon targeting at earlier points along the mammalian visual pathway (e.g., Williams et al., 2006) and with the abovementioned work in chicks and flies showing that N-Cadherin is important for lamina- and target-specificity (Inoue and Sanes, 1997; Lee et al., 2001; Prakash et al., 2005). Future studies that examine cadherin removal selectively in RGCs or in their targets, ought to shed further light on the mechanisms by which cadherins induce circuit specificity. In the meantime, our results provide evidence that cadherin mediated cell-cell adhesion is important for the establishment of functionally precise neural circuits in the mammalian visual system, by ensuring the appropriate sets of neurons in the eye connect to the appropriate sets of target nuclei in the brain.

EXPERIMENTAL PROCEDURES

Animals

Cadherin-3 BAC-EGFP (Cdh3-GFP) mice were obtained from MMMRC. Cdh6-GFP mice were generated as described in Inoue et al., (2009). Cdh6 knockout mice were made as described in Dahl et al. (2002) and obtained from stocks at Jackson laboratories. All procedures were carried out according to protocols approved by animal care and use committees at UCSD, UCSC, Stanford, and NYU.

Immunostaining

Immunostaining for GFP was carried out as described in Huberman et al. (2008) using rabbit anti-GFP (Invitrogen; 1:1000), rabbit anti-melanopsin (ATS; 1:2000), goat anti-ChAT (Chemicon; 1:100), rabbit anti-Cdh6 (Dr. Gregory Dressler University of Michigan; 1:500) or mouse anti-parvalbumin (Chemicon; 1:2000) and Alexa-488, -594, or -647 secondary antibodies.

Labeling of Retinal Ganglion Cell Axons

Methods identical to those described in Huberman et al. (2008) were used. Briefly, a 3 μl volume of 0.5% cholera-toxin beta (diluted in sterile saline) conjugated to Alexa-594 (Invitrogen) was injected into the right and left vitreous of Cdh3-GFP mice using a Hamilton syringe with 33 gauge needle. Twenty-four hours later, the mice were sacrificed, their brains removed and fixed for 24 hr in 4% PFA, then cryoprotected in 30% sucrose and sectioned at 35 μm in either the coronal or sagittal plane.

In Situ Hybridization

Complementary DNAs for Cdh1 (nucleotides 1624–2193 of the mouse mRNA, NM_009864), Cdh2 (nucleotides 2253–2800, NM007664), Cdh3 (nucleotides 836–1356, NM_007665), Cdh4 (nucleotides 530–1273, NM_009867), Cdh5 (nucleotides 722–1293, NM_009868), Cdh6 (nucleotides 202–1229 NM_007666), Cdh7 (nucleotides 1029–1517, NM_172853), and Cdh8 (nucleotides 241–1481, NM_007667) were used to make antisense and sense digoxigenin-labeled RNA probes. In situ hybridization as previously described (Feldheim et al., 1998); protease K treatments were 1 mg/ml for 1 min.

Targeted Intracellular Filling of Ganglion Cells

Cdh3-RGCs were targeted and injected with Neurobiotin in live retinal explants then fixed and reacted with streptavidin-Cy3 (see Völgyi et al., 2009 for details).

Retinal Ganglion Cell Quantification

Cdh3-RGCs were counted from montaged high-resolution photomicrographs and then confirmed in the actual tissue specimen by comparison of the photo montages with the direct view of the retina on a Zeiss M1 microscope at 10–20× magnification. Care was taken to only evaluate retinas where the entire whole mount was obtained by dissection. Student's t tests were used for statistical comparisons of RGC numbers between wild-type and mutant retinae.

SUPPLEMENTAL INFORMATION

Supplemental Information includes four figures and can be found with this article online at doi:10.1016/j.neuron.2011.07.006.

ACKNOWLEDGMENTS

We thank Dr. Gregory Dressler for the cadherin-6 antibody and Tom Clandinin and Maureen Estevez for their helpful suggestions. This work was supported by NIH R01 EY014689 (D.A.F.), NIH R01 EY07360 (S.B.), NIH EY17832 to (B.V.), NIH R21 EY018320 and NIH R01 EY11310 (B.A.B), and NIH R01 EY12793 (D.M.B.) and the E. Matilda Ziegler Foundation for the Blind (A.D.H.).

Accepted: July 11, 2011
Published: August 24, 2011

REFERENCES

Berson, D.M. (2008). Retinal ganglion cell types and their central projections. In The Senses: A Comprehensive Reference, *Volume 1*, Vision 1, T.D. Albright and R. Masland, eds. (San Diego, CA: Academic Press), pp. 491–520.

Bowling, D.B., and Michael, C.R. (1980). Projection patterns of single physiologically characterized optic tract fibres in cat. Nature *286*, 899–902.

Clandinin, T.R., and Feldheim, D.A. (2009). Making a visual map: mechanisms and molecules. Curr. Opin. Neurobiol. *19*, 174–180.

Dahl, U., Sjödin, A., Larue, L., Radice, G.L., Cajander, S., Takeichi, M., Kemler, R., and Semb, H. (2002). Genetic dissection of cadherin function during nephrogenesis. Mol. Cell. Biol. *22*, 1474–1487.

Dickson, B.J. (2002). Molecular mechanisms of axon guidance. Science *298*, 1959–1964.

Ecker, J.L., Dumitrescu, O.N., Wong, K.Y., Alam, N.M., Chen, S.K., LeGates, T., Renna, J.M., Prusky, G.T., Berson, D.M., and Hattar, S. (2010). Melanopsin-expressing retinal ganglion-cell photoreceptors: cellular diversity and role in pattern vision. Neuron *67*, 49–60.

Ellsworth, C.A., Lyckman, A.W., Feldheim, D.A., Flanagan, J.G., and Sur, M. (2005). Ephrin-A2 and -A5 influence patterning of normal and novel retinal projections to the thalamus: conserved mapping mechanisms in visual and auditory thalamic targets. J. Comp. Neurol. *488*, 140–151.

Feldheim, D.A., and O'Leary, D.D. (2010). Visual map development: bidirectional signaling, bifunctional guidance molecules, and competition. Cold Spring Harb. Perspect. Biol. *2*, a001768.

Feldheim, D.A., Vanderhaeghen, P., Hansen, M.J., Frisén, J., Lu, Q., Barbacid, M., and Flanagan, J.G. (1998). Topographic guidance labels in a sensory projection to the forebrain. Neuron *21*, 1303–1313.

Giolli, R.A., Blanks, R.H., and Lui, F. (2006). The accessory optic system: basic organization with an update on connectivity, neurochemistry, and function. Prog. Brain Res. *151*, 407–440.

Godement, P., Salaün, J., and Imbert, M. (1984). Prenatal and postnatal development of retinogeniculate and retinocollicular projections in the mouse. J. Comp. Neurol. *230*, 552–575.

Gong, S., Zheng, C., Doughty, M.L., Losos, K., Didkovsky, N., Schambra, U.B., Nowak, N.J., Joyner, A., Leblanc, G., Hatten, M.E., and Heintz, N. (2003). A gene expression atlas of the central nervous system based on bacterial artificial chromosomes. Nature *425*, 917–925.

Güler, A.D., Ecker, J.L., Lall, G.S., Haq, S., Altimus, C.M., Liao, H.W., Barnard, A.R., Cahill, H., Badea, T.C., Zhao, H., et al. (2008). Melanopsin cells are the principal conduits for rod-cone input to non-image-forming vision. Nature *453*, 102–105.

Harrington, M.E. (1997). The ventral lateral geniculate nucleus and the intergeniculate leaflet: interrelated structures in the visual and circadian systems. Neurosci. Biobehav. Rev. *21*, 705–727.

Hertel, N., Krishna, -K., Nuernberger, M., and Redies, C. (2008). A cadherin-based code for the divisions of the mouse basal ganglia. J. Comp. Neurol. *508*, 511–528.

Honjo, M., Tanihara, H., Suzuki, S., Tanaka, T., Honda, Y., and Takeichi, M. (2000). Differential expression of cadherin adhesion receptors in neural retina of the postnatal mouse. Invest. Ophthalmol. Vis. Sci. *41*, 546–551.

Huberman, A.D., Manu, M., Koch, S.M., Susman, M.W., Lutz, A.B., Ullian, E.M., Baccus, S.A., and Barres, B.A. (2008). Architecture and activity-mediated refinement of axonal projections from a mosaic of genetically identified retinal ganglion cells. Neuron *59*, 425–438.

Huberman, A.D., Wei, W., Elstrott, J., Stafford, B.K., Feller, M.B., and Barres, B.A. (2009). Genetic identification of an On-Off direction-selective retinal ganglion cell subtype reveals a layer-specific subcortical map of posterior motion. Neuron *62*, 327–334.

Inoue, A., and Sanes, J.R. (1997). Lamina-specific connectivity in the brain: regulation by N-cadherin, neurotrophins, and glycoconjugates. Science *276*, 1428–1431.

Inoue, T., Tanaka, T., Suzuki, S.C., and Takeichi, M. (1998). Cadherin-6 in the developing mouse brain: expression along restricted connection systems and synaptic localization suggest a potential role in neuronal circuitry. Dev. Dyn. *211*, 338–351.

Inoue, Y.U., Asami, J., and Inoue, T. (2009). Genetic labeling of mouse rhombomeres by Cadherin-6:EGFP-BAC transgenesis underscores the role of cadherins in hindbrain compartmentalization. Neurosci. Res. *63*, 2–9.

Jeon, C.J., Strettoi, E., and Masland, R.H. (1998). The major cell populations of the mouse retina. J. Neurosci. *18*, 8936–8946.

Lee, C.H., Herman, T., Clandinin, T.R., Lee, R., and Zipursky, S.L. (2001). N-cadherin regulates target specificity in the *Drosophila* visual system. Neuron *30*, 437–450.

Mah, S.P., Saueressig, H., Goulding, M., Kintner, C., and Dressler, G.R. (2000). Kidney development in cadherin-6 mutants: delayed mesenchyme-to-epithelial conversion and loss of nephrons. Dev. Biol. *223*, 38–53.

Masland, R.H. (2001). The fundamental plan of the retina. Nat. Neurosci. *4*, 877–886.

Prakash, S., Caldwell, J.C., Eberl, D.F., and Clandinin, T.R. (2005). Drosophila N-cadherin mediates an attractive interaction between photoreceptor axons and their targets. Nat. Neurosci. *8*, 443–450.

Price, S.R., De Marco Garcia, N.V., Ranscht, B., and Jessell, T.M. (2002). Regulation of motor neuron pool sorting by differential expression of type II cadherins. Cell *109*, 205–216.

Prichard, J.R., Stoffel, R.T., Quimby, D.L., Obermeyer, W.H., Benca, R.M., and Behan, M. (2002). Fos immunoreactivity in rat subcortical visual shell in response to illuminance changes. Neuroscience *114*, 781–793.

Rivlin-Etzion, M., Zhou, K., Wei, W., Elstrott, J., Nguyen, P.L., Barres, B.A., Huberman, A.D., and Feller, M.B. (2011). Transgenic mice reveal unexpected diversity of on-off direction-selective retinal ganglion cell subtypes and brain structures involved in motion processing. J. Neurosci. *31*, 8760–8769.

Scalia, F. (1972). The termination of retinal axons in the pretectal region of mammals. J. Comp. Neurol. *145*, 223–257.

Sperry, R.W. (1963). Chemoaffinity in the orderly growth of nerve fiber patterns and connections. Proc. Natl. Acad. Sci. USA *50*, 703–710.

Suzuki, S.C., Inoue, T., Kimura, Y., Tanaka, T., and Takeichi, M. (1997). Neuronal circuits are subdivided by differential expression of type-II classic cadherins in postnatal mouse brains. Mol. Cell. Neurosci. *9*, 433–447.

Takeichi, M. (2007). The cadherin superfamily in neuronal connections and interactions. Nat. Rev. Neurosci. *8*, 11–20.

Tamamaki, N., Uhlrich, D.J., and Sherman, S.M. (1995). Morphology of physiologically identified retinal X and Y axons in the cat's thalamus and midbrain as revealed by intraaxonal injection of biocytin. J. Comp. Neurol. *354*, 583–607.

Völgyi, B., Chheda, S., and Bloomfield, S.A. (2009). Tracer coupling patterns of the ganglion cell subtypes in the mouse retina. J. Comp. Neurol. *512*, 664–687.

Williams, S.E., Grumet, M., Colman, D.R., Henkemeyer, M., Mason, C.A., and Sakurai, T. (2006). A role for Nr-CAM in the patterning of binocular visual pathways. Neuron *50*, 535–547.